

Central and Reflex Neuronal Responses Elicited by Odor in a Terrestrial Mollusk

R. GERVAIS, D. KLEINFELD, K. R. DELANEY, AND A. GELPERIN

Biological Computation Research Department, Lucent Technologies, Murray Hill, New Jersey 07974

SUMMARY AND CONCLUSIONS

1. We studied the responses to odor of a central olfactory processing organ and subsequent central outputs in the terrestrial mollusk *Limax maximus*. We used extracellular recording techniques and optical recording from preparations stained with a voltage-sensitive dye to characterize network responses in the central organ and whole nerve recording to characterize central odor-elicited outputs.

2. The central olfactory organ, the procerebral (PC) lobe, is a highly interconnected network of local olfactory interneurons that receives input from primary olfactory receptors. In the absence of odor the PC network is known to exhibit periodic waves of excitation and inhibition at a frequency of ~ 0.7 Hz. Here we study how different odor inputs affect the intrinsic oscillatory dynamics.

3. Odor stimulation causes the propagation of electrical activity along the lobe to transiently switch from the state with propagating waves, with typical phase shifts of one half cycle along the lobe, to a state with few or no phase differences along the lobe. The collapse of the phase gradient typically occurs without spatially localized changes in the amplitude of the oscillation, at least on the scale of our optical resolution, ~ 0.1 times the length of the lobe. In some trials, however, we resolved spatial nonuniformities in the magnitude of excitation across the lobe.

4. The collapse of the phase gradient along the lobe in response to odor stimulation is robust on a trial-by-trial basis. Further, the change in phase gradient can occur with little or no change in the frequency of oscillation, as occasionally observed in response to weak odor stimulation.

5. Typically odor stimulation causes changes in the frequency of the oscillation. Two odors, one attractive (potato) and one repellent (amyl acetate), produced different patterns of change; potato induced a transient increase in frequency, whereas amyl acetate produced an initial decrease in frequency followed by a transient increase in frequency. We do not yet know whether these frequency change patterns are unique to these specific odors or to their behavioral meaning.

6. Previous work demonstrated direct connections from the PC lobe to the buccal and pedal ganglia, centers controlling feeding and locomotion, respectively. To establish a correlation between odor-induced changes in the PC lobe and activation of such centers and subsequently effector organs, we recorded from selected central connectives and peripheral nerve roots. The dependence of odor-elicited activity recorded in connectives and nerve roots on PC integrity was assessed by measurements of odor-elicited activity before and after PC ablation.

7. Odor stimulation caused activation of multiple units in the cerebrobuccal connective. One output of the buccal ganglion, the salivary nerve, also showed odor-elicited activation of an identified unit, the slow burster. The necessity of the PC lobe for activation of the slow burster was established by measurements of odor-elicited activity before and after PC ablation.

8. Odor stimulation also caused activation of multiple units in the buccal mass retractor nerve. Activation of a fraction of these

units (3 of 10) was dependent on an intact PC lobe, like the slow burster neuron in the salivary nerve.

9. Our results clearly show how stimuli may lead to changes in the spatial-temporal pattern of activity in a central circuit without changing the overall average level of activity in that circuit.

INTRODUCTION

Coherent network oscillations are a prominent feature of central olfactory processing networks in mammals (Adrian 1942; Freeman 1975), fish (Satou 1990; Thommesen 1978), reptiles (Beuerman 1975), amphibians (Libet and Gerard 1939; Delaney and Hall 1996), arthropods (Laurent and Davidowitz 1994; Laurent and Naraghi 1994), and mollusks (Gelperin and Tank 1990; Kimura et al. 1993; Schütt and Basar 1994; Yamada et al. 1996). The function of oscillatory dynamics in processing olfactory sensory input is not clear (Tank et al. 1994). We are using an oscillatory olfactory network, the procerebral (PC) lobe of the terrestrial slug *Limax maximus*, to investigate the computational role of oscillatory dynamics for sensory processing, in particular odor recognition and categorization.

Odor identity may be encoded in the spatial and temporal pattern of oscillatory activity elicited or modified by activity in the set of receptors responding to ligands in the stimulus (Hildebrand 1994; Kauer 1991; Lancet 1994; Mori and Shepherd 1994). The behavioral relevance of oscillatory activity patterns can be determined from simultaneous measurements of oscillatory activity and odor-signaled behavior (Freeman and Viana Di Prisco 1986) or, in reduced preparations, from odor-elicited reflex responses with clear behavioral meaning, such as the galvanic skin response (Dorries et al. 1994) or nose withdrawal reflex (Chase and Hall 1996; Peschel et al. 1996). Behavioral criteria were essential for successful demonstration of odor-specific spatial amplitude patterns of surface electroencephalogram in rabbit olfactory bulb (Freeman and Schneider 1982; Freeman and Skarda 1985; Gray and Skinner 1988; Viana di Prisco and Freeman 1985).

Ultimately we wish to characterize the transition from odor responses in central neural networks to motor (reflex) outputs reflecting odor-guided behavior. The search for odor-elicited reflex responses in *Limax* is guided by behavioral observations of odor effects on feeding. Behaviorally attractive odors can trigger feeding on plain agar (Sahley et al. 1992), which suggests that such odor inputs provide excitation to elements of the feeding control system (Delaney and Gelperin 1990a–c). In the absence of agar stimulation, attractive odor inputs may activate elements of the feeding motor system in ways detectable with electrophysiological

recording in isolated preparations. We therefore sought odor-elicited reflex outputs in the feeding motor system and elsewhere to determine whether such outputs signaled the behavioral relevance (attractive vs. repellent) of the odor stimulus.

This study has three parts. First, we further characterized (Delaney et al. 1994) the nature of odor-elicited changes in PC lobe activity, with the use of multisite optical and electrical recording. Repeated stimulation with the same set of stimuli allowed analysis of the characteristics and variability in response to a given odor. Second, we characterize responses in motor nerves elicited by attractive and repellent odors. Third, the importance of PC processing for odor-elicited motor responses was tested by comparing responses before and after PC ablation.

Preliminary aspects of this work have appeared in abstract form (Gelperin et al. 1992, 1994).

METHODS

Slugs were obtained from a laboratory colony maintained on a 14:10 light:dark cycle and fed modified Purina rat chow (mix 5010C-9) ad libitum. Animals were anesthetized by cooling with crushed ice for 30 min. The heads were removed and immediately placed in *Limax* saline (Delaney and Gelperin 1990a) maintained at 3°C by a peltier device. The CNS with buccal ganglia and superior tentacles was isolated by fine dissection. The proximal half of the superior tentacle retractor muscle was removed, preserving the olfactory nerve, which runs from the cerebral ganglion to the digitate ganglion inside the cylindrical cavity of the superior tentacle retractor muscle. After the CNS was pinned to the Sylgard base of a preparation dish, the distal tip of the superior tentacle was passed through a hole in the thin wall of a circular (nose) chamber. The superior tentacle retractor muscle plugged the hole in the chamber wall so that saline could be removed from the chamber to expose the nose (Fig. 1). Experiments were conducted at room temperature (20–22°C).

The nose was arrayed for application of odorants delivered in one of two ways. For airborne application of odorants, the nose was first exposed by removing most of the adjacent tentacle skin and then secured to the Sylgard floor of the nose chamber with 0.002-in. tungsten pins inserted through tentacle skin bordering the olfactory epithelium. The nose chamber was drained and the tip of a three-barrel glass puffer pipette was positioned ~2 mm from the receptor surface. Each glass barrel was fixed on a syringe needle connected to a 1-ml syringe containing a strip of filter paper wetted with an odor source. A connector at the back of the syringe barrel delivered air from a peristaltic pump at a flow rate of 0.1 ml/s under the control of electrically actuated valves. Short odor puffs were used to avoid response fatigue. Attractive odor sources were 10⁻⁴% (vol/vol) 2-ethyl-3-methoxypyrazine (EMOP) (Hopfield and Gelperin 1989), mushroom (Gelperin 1975), and rat chow (FOOD). Aversive odor sources were 10⁻³% amyl acetate (AA) (Sahley 1990) and garlic (Sahley et al. 1990), made by soaking 1 g of source material in 100 ml saline for 10 min and then filtering with Whatman #2 filter paper. Odor source solutions were made daily. For AA the concentration given is that of the freshly made solution. One or more attractive and one or more aversive odors were used in each experiment, with no differences in response between attractive and aversive odors for any of the measures of odor activation we used.

The second odor application method used solutions of odorants in saline applied directly to the receptor surface. Initial experiments with aqueous odorant application involved removing most of the saline from the nose chamber and gently adding saline containing odorant. In subsequent experiments, the cylinder of tentacle skin surrounding the nose was cannulated with a plastic tube (1.0 mm

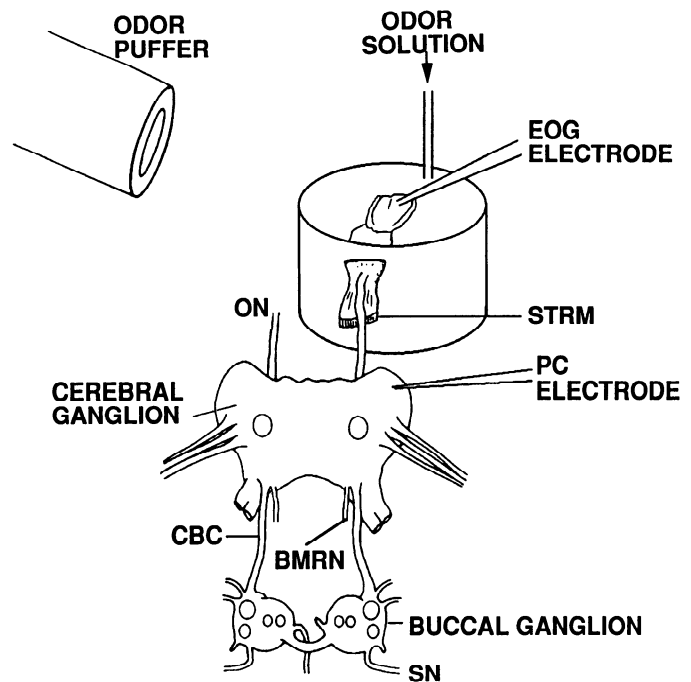


FIG. 1. Diagram of the nose-brain preparation of *Limax* showing how odors are applied to the exposed olfactory sensory epithelium during recording electroolfactogram (EOG) from the receptor surface, field potential oscillation from the procerebral (PC) lobe, and motor nerve activity with suction electrode recording from the salivary nerve (SN), buccal mass retractor nerve (BMRN), or cerebrobuccal connective (CBC). ON, olfactory nerve, STRM, superior tentacle retractor muscle. The nose chamber is drained of saline to expose the receptor surface for odor stimulation. The nose is periodically rinsed with saline.

OD, 0.6 mm ID) sutured in place with its tip adjacent to the sensory epithelium. A second plastic tube (0.3 mm OD, 0.15 mm ID) was placed inside the first tube with the tip of the small inner tube coterminous with the outer tube. Aqueous solutions of odorants were injected via the inner cannula so that they passed over the nose and drained via the outer cannula. Saline injections provided a control for mechanical effects of stimulus application. This method of aqueous odor application did not allow brief stimulation as with odor puffs, so we increased the intertrial interval accordingly.

The electroolfactogram (EOG) response to odor puffs was recorded from the receptor surface with the use of saline-filled glass microelectrodes of 50–100 μ m tip opening and a DC-coupled amplifier. Nerve recordings were made with plastic suction electrodes and AC-coupled amplifiers. The field potential in the PC lobe was recorded with one or two saline-filled patch electrodes of 3–5 μ m tip diam and current-to-voltage conversion using a List EPC-7. All records were digitized at 1 kHz and stored on a computer (Apple MacIIx) for later analysis of activity patterns in different spike amplitude classes.

Optical recordings of voltage-dependent changes at selected regions of the PC lobe used preparations arranged as shown in Fig. 2A after staining with Di-4-ANEPPS (no. D 1199; Molecular Probes, Eugene, OR) (Loew et al. 1992). Care was taken to ensure that the receptor surface was moist but not submerged during stimulus application, and, as in the local field potential measurements, the EOG was recorded during odor application. The dye is prepared as a 1% (wt/vol) stock solution in 70% (vol/vol) ethanol/water and diluted to 0.002% (wt/vol) in *Limax* saline just before use. The preparation is stained at room temperature for ≥ 1 h. The optical system is configured around an inverted microscope with excitation and emission pathways essentially as described in Kleinfeld et al. (1994). We record images of the fluorescent emis-

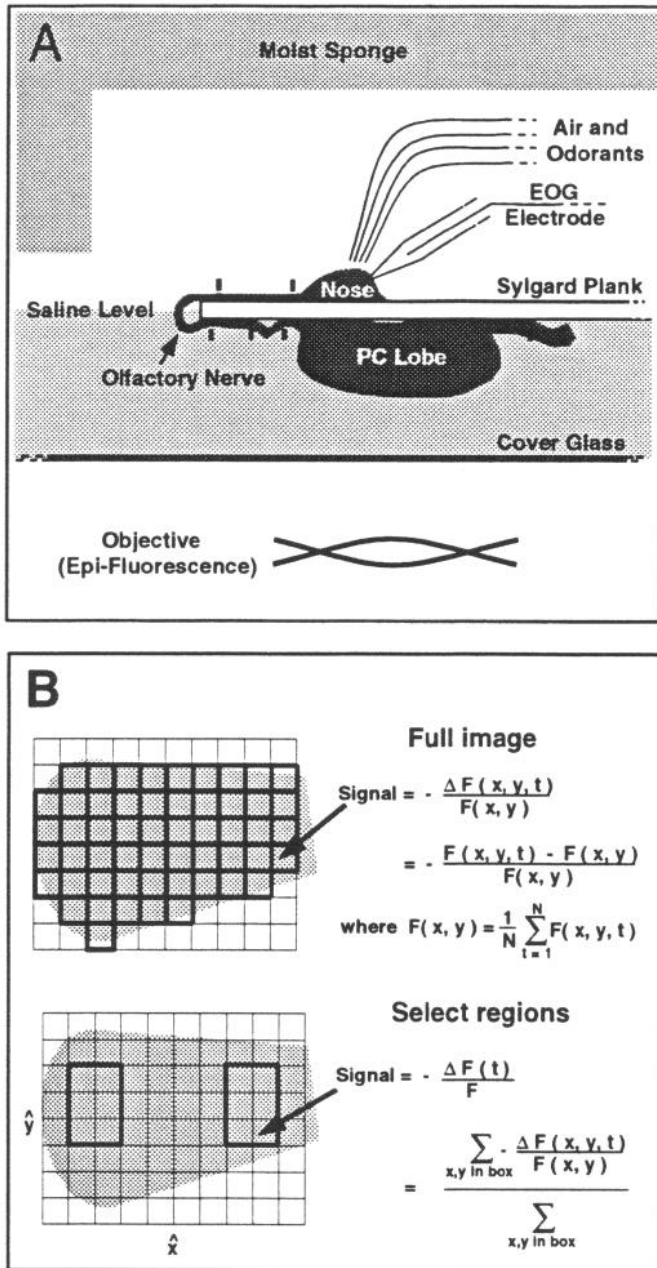


FIG. 2. Preparation and data analysis used for optical recording of odor-evoked activity in the PC lobe. *A*: nose and PC lobe are pinned on opposite sides of a wafer of Sylgard, with a sponge suspended above the nose to retard dessication. Use of low concentrations of attractive odors minimized odor-induced movement artifacts. *B*: images were analyzed as sequences of pixel values and displayed as movies or plots of pixel values binned from distal and proximal areas of the PC lobe.

sion from the PC lobe with a charge coupled device (CCD) camera (model CH220 with Thomson 7883 detector, 500 kHz 12-bit analog-to-digital converter and NuBus interface; Photometrics, Tucson, AZ) under the control of a Macintosh IIfx computer (Apple, Cupertino, CA). The camera operates in frame-transfer mode (Lasser-Ross et al. 1991) and acquires consecutive images of the entire field with a typical resolution of $6 \mu\text{m}$ per pixel for a 100×100 pixel image at a frame rate of 13 Hz. The intensity in each frame is denoted $F(x, y, t)$. The average voltage change in each pixel is linearly proportional to the fractional change in the measured emission, i.e., $\Delta V(x, y, t) \propto -\Delta F(x, y, t)/F(x, y)$, as defined for the full image in Fig. 2*B*. We plot also $-\Delta F(t)/F$, the fractional

change averaged over several pixels at selected regions in space, also shown in Fig. 2*B*.

The spatial coherence across the lobe is quantified in terms of the correlation coefficient between measurements at distal (D) and proximal (P) sites. The correlation coefficient, denoted $C_{DP}(t)$, is computed as a running average over one period of the oscillation of the local field potential or optical signal, i.e.

$$C_{DP}(t) = \frac{\langle \delta S_D(t) \delta S_P(t) \rangle}{\sqrt{\langle \delta S_D^2(t) \rangle \langle \delta S_P^2(t) \rangle}} \quad (1)$$

where $\delta S(t)$ refers to the change in the signal, $S(t)$, relative to its mean value, i.e.

$$\delta S(t) \equiv S(t) - \langle S(t) \rangle \quad (2)$$

and the brackets $\langle \cdot \cdot \cdot \rangle$ denote time averaging, defined as

$$\langle S(t) \rangle = \frac{1}{T} \int_{t-T/2}^{t+T/2} dx S(x) \quad (3)$$

where $T \equiv 1/\nu_0$ is the period. In practice, the integral is computed as a discrete sum over digitized data. $C_{DP} = +1$ corresponds to an identical temporal response at both distal and proximal sites, irrespective of differences in absolute magnitude. The value of the correlation function will depend on the shape of the waveforms as well as their relative timing and thus should be understood to be a qualitative measure. For spikes, C_{DP} is 0 until the relative time difference is less than the spike width. For sinusoids, $C_{DP} = +1$ corresponds to a phase difference of 0, $C_{DP} = 0$ corresponds to a phase difference of a quarter cycle, and $C_{DP} = -1$ corresponds to antiphasic oscillations, i.e., a phase difference of a half cycle.

RESULTS

Central responses

To determine that odors delivered to the nose activated receptors and initiated input to the PC lobe, we measured EOG responses at the nose and field potential responses in the PC lobe simultaneously while applying 4 s puffs of air, EMOP, or AA onto the nose (Fig. 3). At a velocity of 0.1 ml/s, moist air had no effect (Fig. 3*A*). Both AA and EMOP produced a slow negative-going EOG and changes in PC oscillation frequency (Fig. 3, *B* and *C*). Note that the intensity of the PC response did not scale with the amplitude of the EOG, a consistent finding.

To assess the nature of the PC oscillation frequency changes produced by AA and EMOP, a group of trials (3 preparations, each given 2–5 trials with all 3 odors) containing responses to 4-s puffs of air ($N = 13$), $10^{-4}\%$ (vol/vol) AA ($N = 12$), and $10^{-4}\%$ (vol/vol) EMOP ($N = 11$) were analyzed in the following way. For each odor application trial, the 10 cycles of field potential oscillation preceding stimulus onset were measured to determine the mean preodor frequency, ν_0 . Then, for each of the 20 cycles following odor onset, the instantaneous frequency was determined and the fractional change in frequency was computed on a cycle-by-cycle basis as

$$\frac{\Delta \nu}{\nu_0} \equiv \frac{\nu_{\text{nth cycle}} - \nu_0}{\nu_0} \quad (4)$$

This presentation emphasizes changes from the preodor baseline frequency in response to odor stimulation (Fig. 4, *top, middle, bottom*). The PC oscillation frequency response to air showed only small changes, perhaps due to mechanical aspects of the stimulus. The pattern of oscillation change for EMOP stimulation was predominantly an increase in

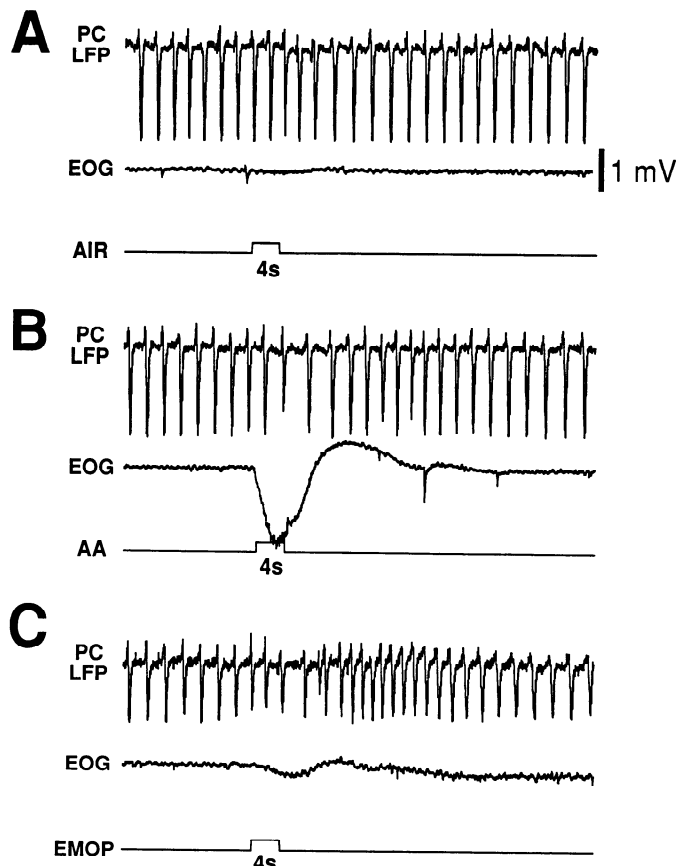


FIG. 3. Field potentials recorded in the PC lobe and EOG responses recorded from the sensory epithelium of the nose in response to 4 s puffs of (A) moist air (AIR), (B) amyl acetate (AA), and (C) 2-ethyl-3-methoxy pyrazine (EMOP).

frequency, with some indication of a transient decrease in frequency early in the response [Fig. 4, *middle*, 3rd cycle after stimulus onset (cycle 13); Fig. 3C, 3rd cycle after stimulus onset]. The PC response to AA was characterized by an initial decrease in oscillation frequency for four to five cycles followed by a rebound increase in frequency and return to baseline. These patterns are evident in the records of Fig. 3. Statistical analysis by pairwise comparisons of the responses to air, EMOP, and AA indicates a significant difference between them in each case (F test, $P < 0.05$ for air vs. EMOP, air vs. AA, and EMOP vs. AA).

We observed some responses to weak odors different than simple shifts in frequency. An initially irregular oscillation could be regularized by the odor pulse (Fig. 5A) or a regular oscillation made irregular by the odor pulse (Fig. 5B). Strong odor stimulation, particularly with AA, could change the frequency and waveform of the oscillation dramatically (Fig. 5C). We generally avoided strong odor stimuli and, with one exception (Fig. 8), have not included in the analysis presented here the $\sim 20\%$ of weak odor trials that changed the regularity of the waveform. Changes in waveform of the oscillation triggered by odor stimulation may be an important aspect of odor recognition and classification, but appropriate analytical methods have not yet been applied.

To examine electrophysiologically the spatial aspects of odor effects on PC activity, we made simultaneous two-site recordings of the PC local field potential during odor stimulation. Two types of spatial comparisons were made,

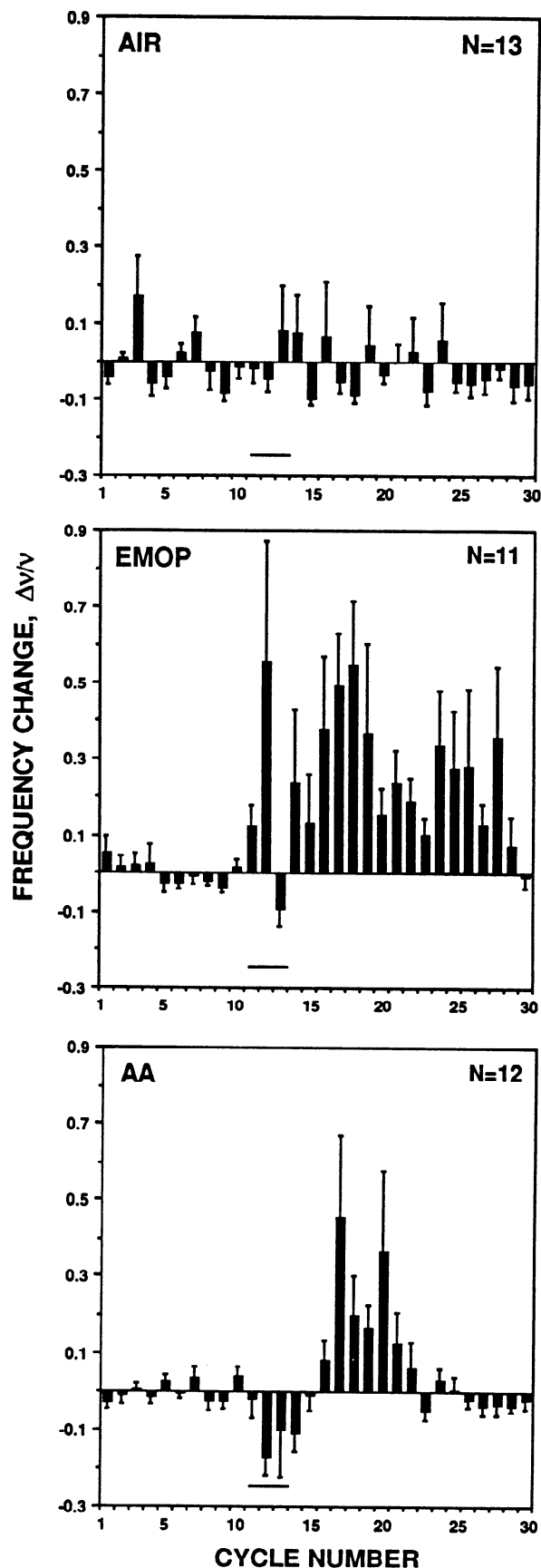


FIG. 4. PC oscillation frequency changes in response to air, EMOP, and AA. The data are binned by cycle number for all trials of a given odor and averaged, with the number of trials indicated in the *top right corner*. Stimulus duration was 4 s for all trials, indicated by a horizontal line starting at cycle 11.

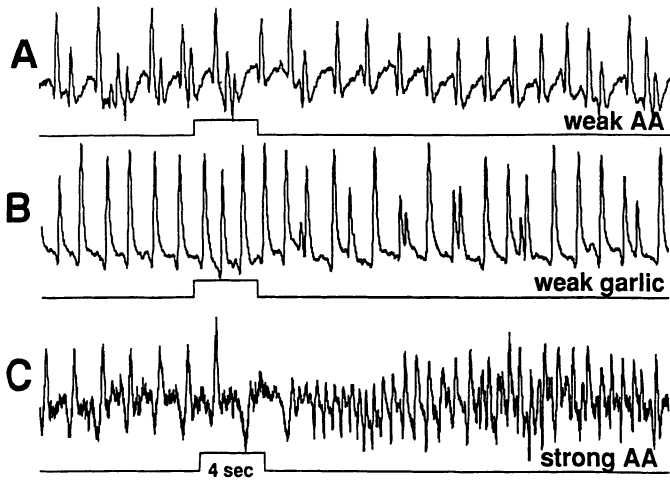


FIG. 5. Pattern of field potential oscillation can be altered by odor stimulation. *A*: weak AA stimulus transiently regularizes an irregular PC rhythm. *B*: weak garlic odor stimulus transiently causes irregularity in a previously regular PC rhythm. *C*: strong AA stimulus changes the pattern and waveform of the PC oscillation for tens of seconds.

with electrodes either $150\ \mu\text{m}$ apart but at the same level on the distal-proximal axis of the PC or separated by $150\ \mu\text{m}$ along the distal-proximal axis (Fig. 6*A*). Before and during 4-s odor puffs, recordings from sites at the same level on the distal-proximal axis showed very similar responses in terms of oscillation frequency, waveform, and synchrony of peaks between the two sites (data not shown). Recordings from sites separated by $150\ \mu\text{m}$ along the distal-proximal axis of the PC showed that the odor-elicited frequency changes were identical. However, the relative timing of the field potential peaks at the two sites decreased during odor stimulation and led to a transient increase in spatial coherence, shown as an increase of the correlation coefficient (Eq. 1–3) during odor stimulation with garlic (Fig. 6*B*) and EMOP (Fig. 6*C*). The odor-elicited increase in spatial coherence along the distal-proximal axis occurred even if the frequency change elicited by the odor puff was very small (cf. Fig. 6*C* in Delaney et al. 1994) or absent. The time delay (the correlation coefficient and the time delay, Δt , are approximately related by $C_{DP} = \cos 2\pi\nu_0\Delta t$ on a cycle-by-cycle basis) between the peak of the field potential event at two recording sites $\geq 150\ \mu\text{m}$ apart along the distal-proximal axis was compared before and during stimulation with air, EMOP, and AA (15–19 trials, 8 preparations). Significant reductions in time delay were found for EMOP (127 ± 18 ms, mean \pm SE, preodor vs. 87 ± 12 ms, mean \pm SE, in odor, $t = 1.86$, $df = 14$, $P < 0.04$) and AA (126 ± 13 ms preodor vs. 91 ± 9 ms in odor, $t = 2.28$, $df = 18$, $P < 0.04$) but not for air (107 ± 10 ms preodor vs. 103 ± 11 ms in odor, $t = 0.23$, $df = 14$, $P = 0.39$). Thus the change in time delay of the PC oscillation peak can signal odor and not wind, but does not differentiate between behaviorally attractive or repellent odors.

To achieve more localized measurements of PC electrical activity and greater sensitivity to phase gradients along the distal-proximal axis, we performed optical imaging measurements on PC lobes stained with voltage-sensitive dye. We consider first data indicative of the typical response to weak odors, i.e., EMOP at $10^{-5}\%$ (vol/vol). Before delivery of odor the lobe shows waves of depolarization (Fig. 7*A*, red

bands) and hyperpolarization (Fig. 7*A*, purple bands) that propagate from the distal to proximal pole. As previously discussed (Kleinfeld et al. 1994), each wave observed optically corresponds to one cycle of the field potential oscillation. A 5-s EMOP stimulus to the exposed superior nose causes the phase delay between peak depolarization at the distal and proximal poles to decline markedly (Fig. 7*A*, cycles 3–5) such that activity throughout the lobe transiently switches from a wave-propagating state to a nearly spatially uniform state (*). Recovery to normal wave propagation occurs within one cycle after stimulus offset (Fig. 7*A*, cycles 6 and 7). Graphs of fluorescent intensity within localized regions at the distal and proximal poles of the PC lobe show the odor-induced collapse of the phase gradient clearly (Fig. 7*B*). As with the two-site measurements of local field potential, a continuous measure of the timing between activity at distal and proximal sites is given by $C_{DP}(t)$, the correlation coefficient between the fluorescent signals from the two sites (Fig. 7*C*). Starting from a quarter cycle out of phase, with $C_{DP} = 0$, this correlation measure shows the gradual increase in spatial coherence throughout the application of the odor. The large change in $C_{DP}(t)$ seen here, compared with that shown for the electrical records (Fig. 6), results from the relatively large separation distance between recording sites in the optical analysis and possibly also from the greater spatial localization of the optical signal versus the local field potential measurement.

Optical recording of a PC response during which both waveform and frequency of the oscillation change is shown

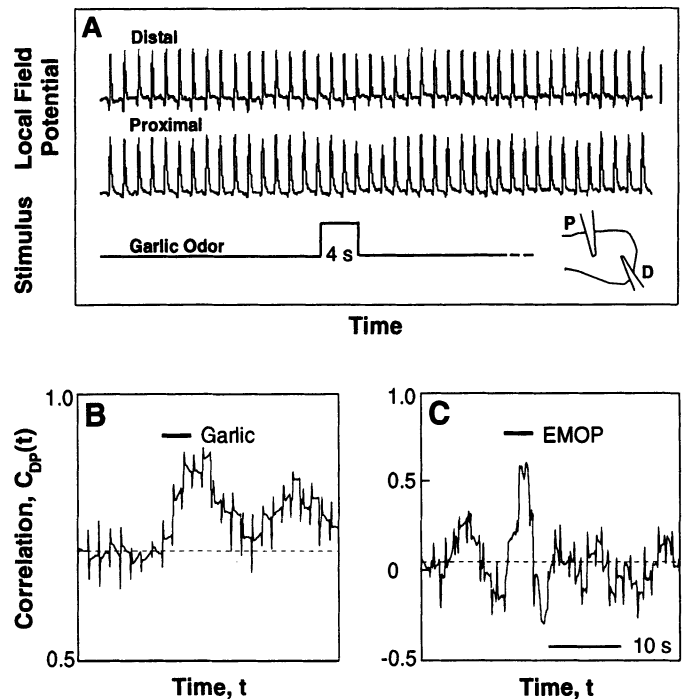


FIG. 6. Odor stimulation affects the relative timing of the local field potential recorded at 2 sites $150\ \mu\text{m}$ apart along the distal-proximal axis of the PC. *A*: top record is from a distal site (D); bottom record is from a proximal site (P), as shown in the inset. *B*: cross-correlation (Eq. 1–3) of the waveforms in *A* shows an increase in coherence in response to garlic odor stimulation. Dashed line corresponds to the prestimulation baseline. *C*: cross-correlation of field potential waveforms recorded from 2 sites as in *A*, but with EMOP stimulation. Dashed line corresponds to the prestimulus baseline.

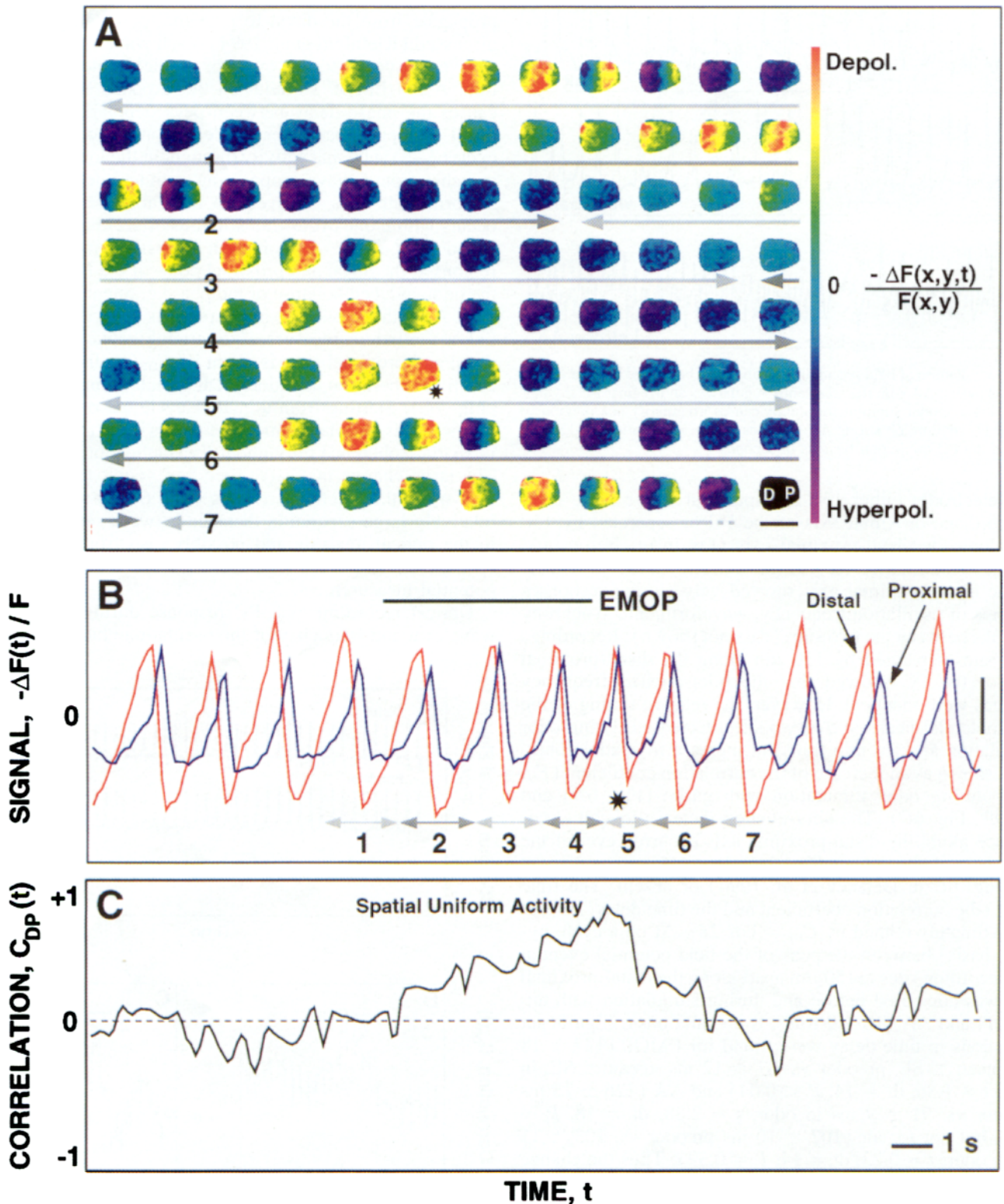


FIG. 7. Optical recording of PC response to an odor stimulus that transiently increased the PC oscillation frequency and led to spatially uniform electrical activity. **A**: continuous image sequence that shows activity before, during, and after presentation. Arrows: successive periods of the oscillation. Odor application starts at the end of period 1. The maximum increases in both frequency and spatial coherence ($*$) occur in period 5. Scale bar under last frame: $500 \mu\text{m}$. **B**: graphs of average fluorescence within 10×30 pixel regions at the distal and proximal poles of the PC lobe. Locations of binned areas are shown in the last frame of **A** by symbols D (distal) and P (proximal). Scale bar corresponds to $|\Delta F/F| = 2 \times 10^{-4}$. Arrows: cycles shown in **A**. **C**: equal-time cross-correlation coefficient between the distal and proximal signals shown in **B**. The correlation is calculated as a continuous function of time with an averaging interval of 1 cycle.

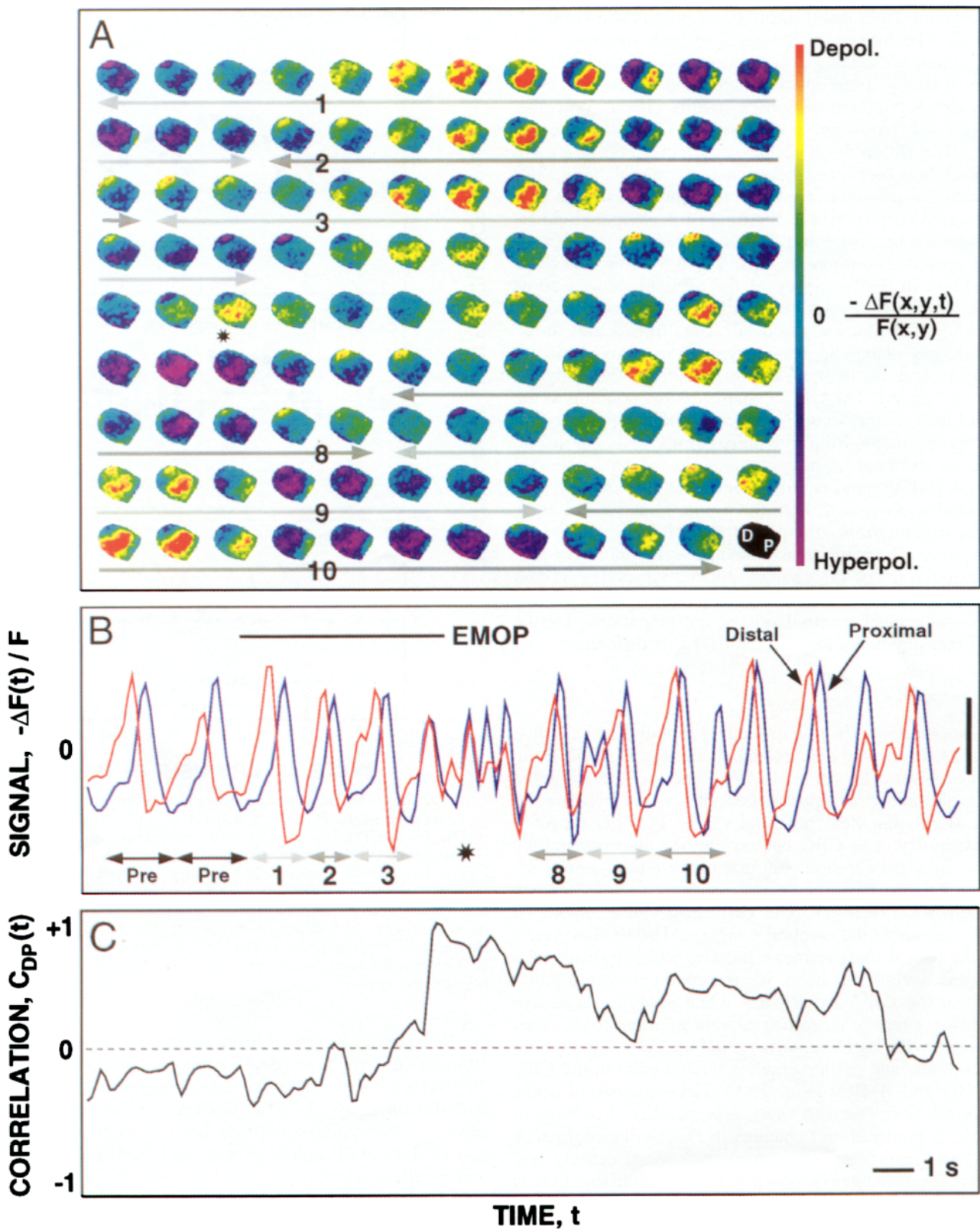


FIG. 8. Optical recording of PC response to an odor stimulus that altered PC oscillation waveform and frequency. *A*: continuous image sequence that shows activity before, during, and after odor presentation. Arrows: successive periods of the oscillation. Odor application starts at the beginning of period 1. The maximum increases in both frequency and spatial coherence occur in the epoch denoted with an asterisk; note the localized punctate responses. Scale bar under last frame: $500 \mu\text{m}$. *B*: graphs of average fluorescence within 10×30 pixel regions at the distal and proximal poles of the PC lobe. Locations of binned areas are shown in the last frame of *A* by symbols D (distal) and P (proximal). Scale bar corresponds to $|\Delta F/F| = 1 \times 10^{-4}$. Numbered arrows: cycles shown in *A*. *C*: equal-time cross-correlation coefficient between the distal and proximal signals shown in *B*. The correlation is calculated as a continuous function of time with an averaging interval of 1 cycle.

in Fig. 8A. The preodor pattern of bandlike propagation of depolarization from distal to proximal pole is shown in cycles 1–3. The maximum increases in both frequency and spatial coherence occur just before and after stimulus offset, seen most clearly in the epoch denoted with an asterisk. Note the localized punctate responses in this epoch. Wavelike propagation is recovered in cycles 6–7. Graphs of average fluorescence within distal and proximal sites (Fig. 8B) and the correlation coefficient between these signals (Fig. 8C) show that the transient frequency maximum in the fluorescence signal corresponds to the time of peak spatial coherence between the distal and proximal sites.

The optical recordings in Figs. 7 and 8 show that there are changes in the frequency of the oscillations as well as changes in phase in response to EMOP. We now consider such changes in frequency in detail. Data from a trial showing the largest change in frequency, both in terms of magnitude and duration, in our sample of optical recordings is shown in Fig. 9A. The typical change, corresponding to the data in Fig. 7, is shown in Fig. 9B, and the composite result for 12 measurements from five preparations is shown in Fig. 9C. As in the case of measurements based on local field potential, EMOP induces only an increase in frequency. The increase is equivalent at both the proximal and distal ends, with the exception of an expected “glitch” at cycle 2 (see DISCUSSION). The magnitude of change seen optically, ~ 0.2 , and the duration of the change, about four cycles, is less than that seen in the set of local field potential measurements; greater mechanical manipulation of the preparation for the optical measurements may account for this difference.

Reflex responses

To assess odor activation of feeding or withdrawl circuits, we recorded from the cerebrobuccal connective (CBC), the buccal mass retractor nerve (BMRN) and the salivary nerve (SN) while applying aqueous odorants to the nose for 30 s. The oscillating field potential of the PC was recorded simultaneously. The CBC conveys axons of commandlike neurons from the cerebral ganglion to the motor centers for ingestive feeding movements in the buccal ganglia (Delaney and Gelperin 1990a–c). The CBC also carries axons of buccal neurons to the cerebral ganglion. The BMRN innervates the buccal mass retractor muscle, which positions the buccal mass within the head. We recorded from the cerebral origins of the CBC and BMRN while applying attractive (rat chow) or repellent (garlic) odorant solutions to the nose. Compared with baseline activity before odor stimulation, both rat chow and garlic stimuli activated units in the CBC (Fig. 10) and BMRN (Fig. 11A). Odor-stimulated nerve activity can occur with (6 trials, 3 preparations) or without (8 trials, 3 preparations) changes in PC oscillation rate. A preparation showing both odor-evoked nerve activity and PC oscillation changes is shown in Fig. 10. Note that FOOD odor increased PC oscillation frequency (Fig. 10B), whereas garlic odor produced a biphasic change in PC oscillation frequency (Fig. 10D).

The nature of odor-stimulated activity in the nerve recordings was quantified by taking 60-s samples of record before and during odor stimulation and sorting all spikes above a threshold set at twice the noise level into size classes. The largest-amplitude action potential in the CBC, called

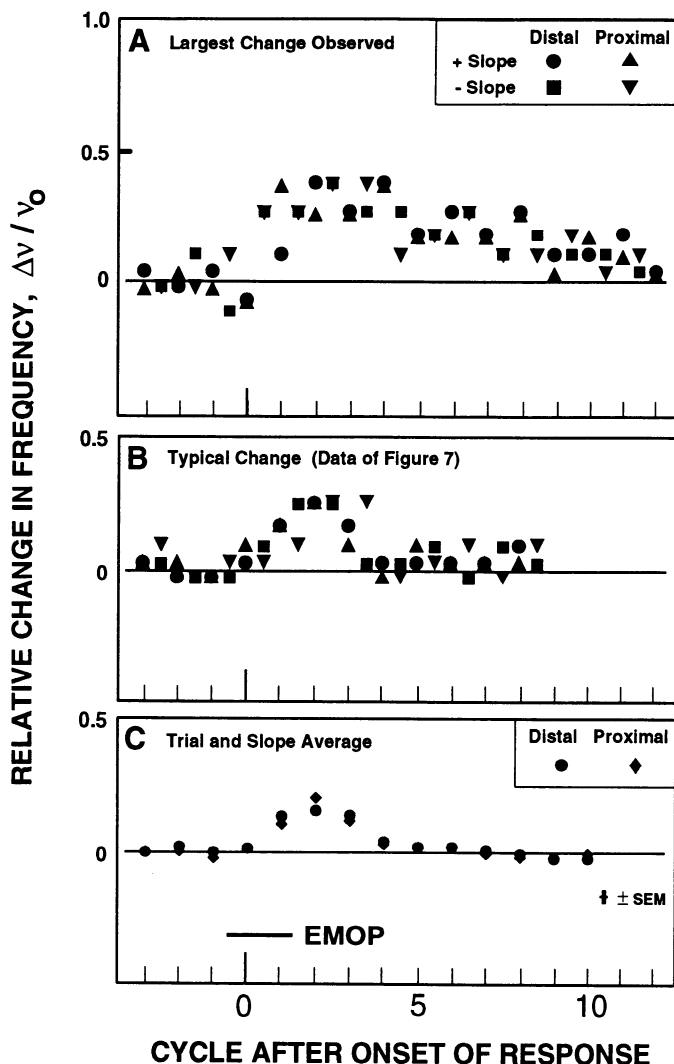


FIG. 9. Transient increase in frequency of oscillation between distal and proximal poles of the PC lobe in response to application of EMOP. We plot the fractional change deduced from optical recordings. The frequency is found from 0 crossings of the signal, and the 4 estimates per cycle correspond to crossings with positive and negative slopes at the distal and proximal poles. The 1st cycle on the abscissa corresponds to the onset of odor-induced change. *A*: result from the preparation that showed the largest increase in terms of both amplitude and duration. *B*: result for the data shown as the image sequence in Fig. 7. *C*: average of the results from 12 odor presentations with 5 different preparations. Mean \pm SE is within the height of the symbols.

cell 1, increases its rate of firing in response to aqueous odor stimulation of the nose (5 of 7 trials on 2 preparations) (Fig. 10). The maximal rate increase was often delayed from stimulus onset by 15–20 s. The response of *cell 1* and the responses of smaller-amplitude units evident in Fig. 10, *B* and *D*, did not differentiate between behaviorally attractive and repellent odors.

Odor application also activated multiple units in the buccal mass retractor (BMR) (Fig. 11A), again with no clear differentiation in response pattern or magnitude between attractive and repellent odors (data not shown). To investigate the dependence of the BMR multiunit response on odor processing by the PC, responses were compared before (Fig. 11*Ba*) and after (Fig. 11*Bb*) PC ablation. We were careful to cut the PC transversely in a way that left between one

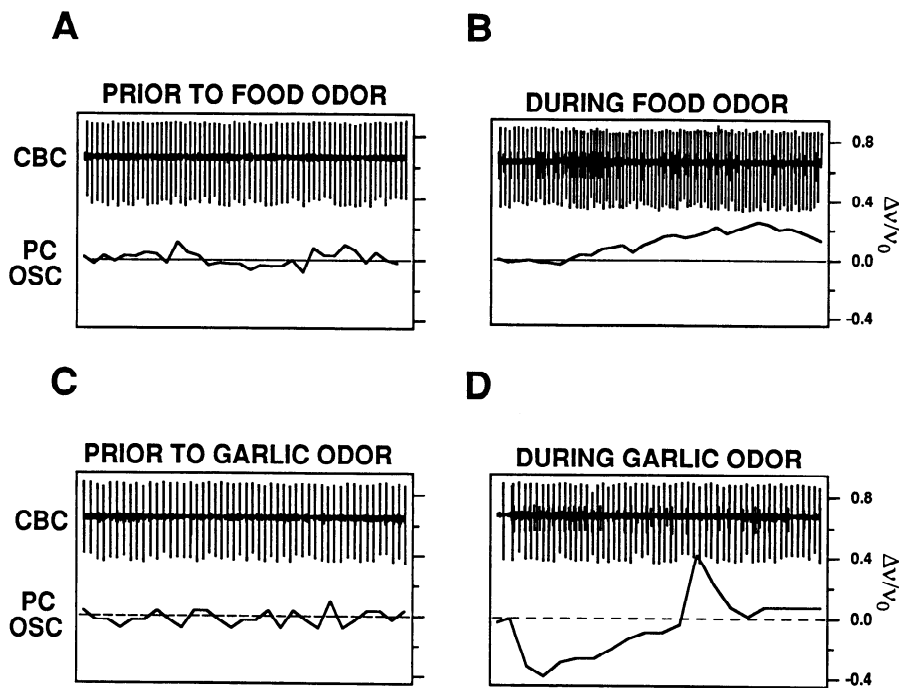


FIG. 10. Activation of units in the CBC and changes in PC lobe oscillation frequency in response to aqueous odors. *A* and *B*: attractive odor (rat chow food) applied to the nose activates *cell 1*, the unit with the highest amplitude, and a number of units with lesser amplitude. PC oscillation frequency is also increased. *C* and *D*: same pattern of CBC activation was seen with garlic, a repellent odor; however, PC oscillation frequency showed a biphasic change. All CBC traces and PC oscillation frequency graphs show 30 s of data immediately after aqueous odor application.

fourth and one third of the proximal portion of the PC intact. This minimizes but does not eliminate the possibility of damage to afferent olfactory pathways. To partially control for nonspecific debilitation due to PC ablation, a third odor stimulation was performed using the nose contralateral to the ablated PC, without moving the recording electrodes (Fig. 11*Bc*). The nose used for stimulation was switched, but not the BMR nerve from which the recording was made. PC ablation reduced but did not eliminate the nerve response to odor, which was restored by odor stimulation of the nose contralateral to the ablated PC. Suppression of large-amplitude units and truncation of the duration of the odor-elicited activity after PC ablation are especially clear. When the spikes are clustered according to their amplitude, 3 of the 10 spike clusters present in the BMR whole nerve response were affected by PC ablation in a manner reversed by stimulation of the contralateral nose (Fig. 11*C*). This result was obtained with three preparations.

The salivary nerves contain axons of several autoactive neurons strongly modulated during fictive feeding (Cope land and Gelperin 1983; Prior and Gelperin 1977). Two units are particularly prominent in SN recordings, the fast salivary burster and the slow salivary burster (Fig. 12*A*). Activity in the fast salivary burster and slow salivary burster was measured before, during, and after garlic and mushroom stimulation of the nose and then remeasured after PC ablation ipsilateral to the nose used for stimulation. Only the slow salivary burster, and not the fast salivary burster, showed an odor-elicited increase in activity that was eliminated by PC ablation (Fig. 12*B*). For mushroom odor with PC intact, analysis of slow burster spikes per trial during 30-s trials before, during, and after odor application showed 40 ± 14 , 71 ± 18 , and 38 ± 17 spikes per trial (mean \pm SE, 3 trials, 2 preparations in all cases). For garlic odor with PC intact, the comparable figures were 31 ± 9 , 55 ± 33 , and 46 ± 18 spikes per trial. Thus an odor-elicited increase in activity in

the SN is clear for attractive stimuli although unclear for aversive stimuli, not inconsistent with results for the BMR response. PC ablation on the same side of the brain as the stimulated nose eliminated the odor augmentation of slow burster activity (32 ± 8 spikes per trial pre-cut vs. 34 ± 15 spikes per trial post-cut). Stimulation of the contralateral nose returned the response to 51 ± 21 spikes per trial. The response to the contralateral nose was larger than the initial response to the ipsilateral nose because the ipsilateral nose had been stimulated previously whereas the contralateral nose has not been stimulated previously.

DISCUSSION

Central responses

The data presented here and in Delaney et al. (1994) document with both optical imaging techniques and electrophysiological recordings that odor stimulation transiently interrupts the wavelike propagation of depolarization from distal to proximal poles in the PC lobe. During odor stimulation PC cells depolarize and hyperpolarize in virtual synchrony throughout the entire structure. This collapse of the phase gradient along the distal-proximal axis is caused by both behaviorally attractive and repellent odors but not moist air puffs. This macroscopic change in spatial activity pattern therefore signals the presence of odor but does not signal the nature of the odor. A limited sample of photodiode measurements of activity at multiple sites during odor stimulation shows that local regions of the PC can decouple from the coherent oscillation and show activity independent of the overall oscillation for a few seconds (Delaney and Kleinfeld, unpublished data). Optical imaging of the PC oscillation response to odor input with finer spatial resolution than the images shown here will be used to look for odor coding by unique spatial patterns of activity in the PC.

A transient phase shift across the length of the PC lobe must be accompanied by a concomitant change in frequency,

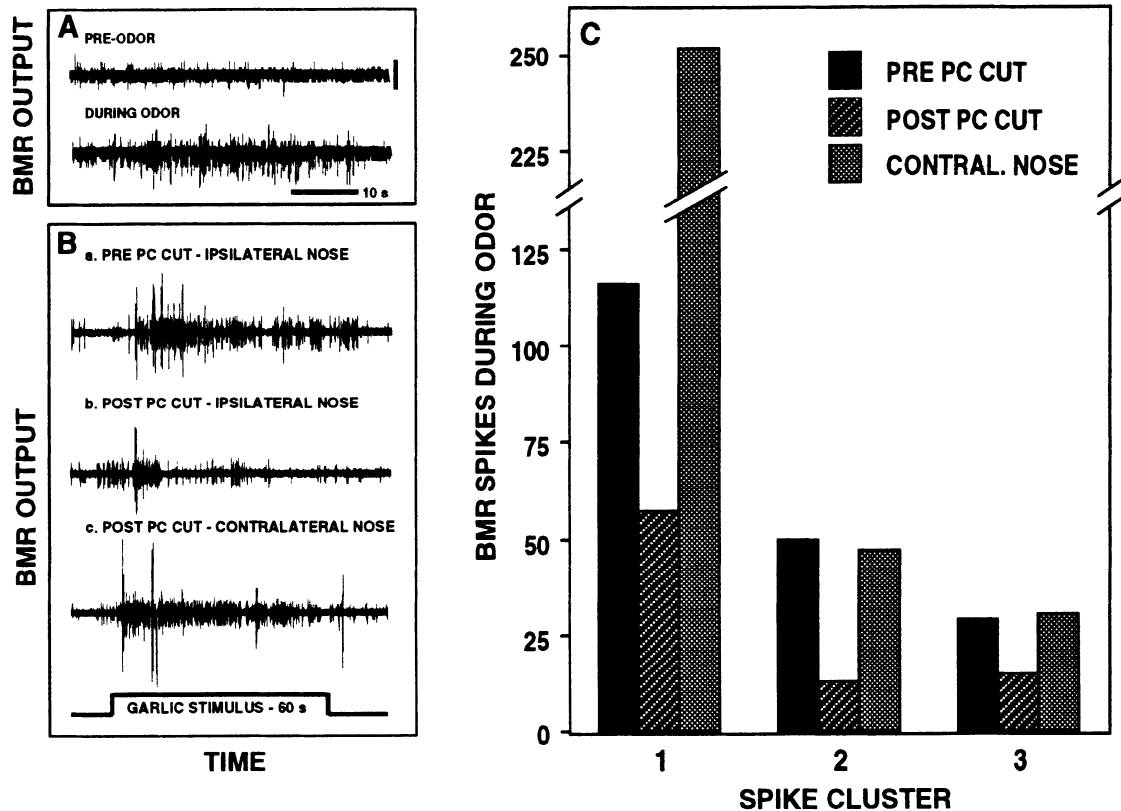


FIG. 11. Odor stimulation activates units in the buccal mass retractor (BMR) nerve, with activity in some units dependent on an intact PC lobe. *A*: activity in the BMR is shown before and during application of rat chow odor. *B*: effect of PC ablation on odor-elicited responses in the BMR nerve. *Ba*: activation of multiple units in the BMR by garlic odor. *Bb*: ablation of the PC ipsilateral to the stimulated nose greatly reduced the odor-elicited activity in the BMR. *Bc*: activation of the BMR by garlic odor is restored by stimulation of the nose contralateral to the recorded BMR. *C*: clustering of spikes by amplitude identified 3 clusters in the BMR response to odor that were maximally affected by PC ablation.

whose sign and magnitude will vary along the length of the lobe. For the present case of wave fronts that propagate distally to proximally with measured phase differences $\Delta\phi_{DP}$ 0.2 cycles (e.g., Fig. 7), the relative shift in frequency between the proximal and distal regions is expected to be $\Delta\nu_{DP}/\nu_o = \Delta\phi_{DP} \cong 0.2$. The observed shift in phase is typically spread over four cycles (Fig. 7), so naively we expect a frequency shift of $\Delta\nu_{DP}/\nu_o \cong 0.05$ per cycle, with the proximal region leading as the phase gradient collapses and then trailing as the phase gradient is reestablished. In practice, for stimulation with EMOP, we observe that both ends of the PC lobe show similar frequency shifts and that the maximum value of the shift, $\Delta\nu/\nu_o = 0.2-0.5$ (Figs. 4 and 7), is much greater than that predicted to accompany the collapse of the phase difference. Thus the transient increase in the frequency of the oscillation is largely independent of the decrement in phase difference along the lobe. On the other hand, the observed frequency shift at the proximal versus distal regions is significantly different, with the expected sign for a phase collapse for one cycle following presentation of EMOP (cycle 2, $\Delta\nu_{DP}/\nu_o = 0.045 \pm 0.025$, Fig. 9C). A relative frequency shift in the opposite direction is, unfortunately, not resolved when the phase gradient reforms; presumably the variability in the timing of the response between trials obliterates this effect (cf. Fig. 9, A and B).

In addition to a possible spatial coding of odor quality, the results from the present study raise the question of frequency coding. Each of the two odorants used elicited a reproducible

pattern of frequency changes that differed significantly from each other and from air. It is clear that further experiments using a larger set of odorant stimuli in a wide concentration range are required to evaluate the importance of frequency changes for odor coding. Many attractive odors change hedonic quality above some critical concentration, changing from attractive to repellent. On the basis of previous behavioral work we have chosen odor concentrations such that EMOP should be attractive and AA aversive. If, however, the biphasic change in oscillation frequency measured in response to AA stimulation is a signature of evaluation as aversive by the PC circuit, then an EMOP stimulus strong enough to be aversive, roughly 100 times stronger than used in this work, should also produce a biphasic change in oscillation frequency.

Differential changes in the PC oscillation frequency caused by different odors could result from differential activation of olfactory receptors. In vertebrates, glutamate is the most likely candidate transmitter mediating sensory cell to mitral/tufted cell synapses (Berkowicz et al. 1994; Didier et al. 1994; Sassoe-Pognetto et al. 1993). Glutamate may be a sensory neurotransmitter in *Limax*, on the basis of observations of intense glutamate-like immunoreactivity of fibers in the olfactory nerve (Gelperin, unpublished data). Similarly, nitric oxide may be involved in olfactory sensory activation (Breer and Shepherd 1993, but see Roskams et al. 1994). Given that exogenous glutamate application decreases the *Limax* PC oscillation frequency (Gelperin et al.

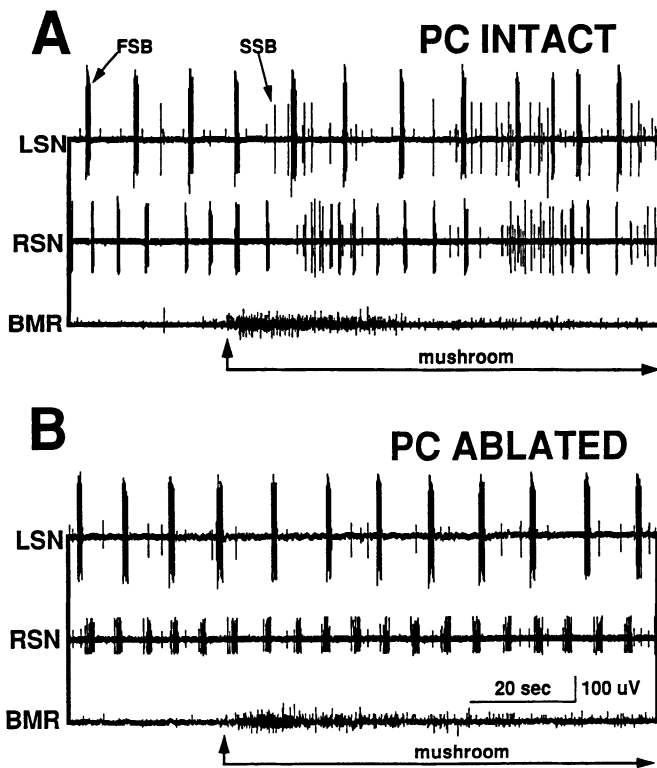


FIG. 12. Activation of units in the SNs by mushroom odor applied to the nose is decreased by ablation of the PC lobe ipsilateral to the stimulated nose. *A*: activity in the left and right SNs (LSN, RSN) and in the BMR nerve elicited by application of mushroom extract. *B*: reduction in mushroom-odor-elicited activity caused by PC ablation ipsilateral to the stimulated nose.

1993), whereas nitric oxide increases it (Gelperin 1994), differential activation of receptor cells containing either glutamate or nitric oxide could result in frequency changes like those in Fig. 3, *B* and *C*.

Oscillations in field potential of olfactory centers or membrane potential of second- or third-order olfactory interneurons have been found in insects (Laurent and Davidowitz 1994; Laurent and Naraghi 1994), crustaceans (Mellon et al. 1992), mollusks (Delaney et al. 1994; Schütt and Basar 1994; Yamada et al. 1996), fish (Satou 1990), and mammals (Haberly 1990; Kay and Freeman 1994; Skinner et al. 1990). The computational significance of oscillatory activity is not yet clear (Tank et al. 1994). Description of the readout mechanism that relays information processed by the oscillating PC network will provide an important constraint on models of olfactory circuit dynamics (Freeman 1991; Hopfield 1991). A set of pedal cells with dendrites in the PC lobe (Chase and Tolloczko 1989) has been recorded after labeling their dendrite in the PC with DiI (1,1'-didodecyl-3,3,3',3'-tetramethylindocarbocyanine perchlorate) (Gelperin et al. 1996). Stimulated activity in PC-connected pedal cells does not alter the PC oscillation; however, nitric oxide activation of the PC (unpublished observations) activated bursts of spikes in the pedal cells. Elucidation of the anatomy of the pedal cell dendrites in the PC and their response to odor stimulation of the nose will provide insight into the readout of olfactory oscillation in *Limax*.

Reflex responses

The results presented here show that odors can elicit activity in output pathways from the cerebral and buccal ganglia

and that some components of the odor-elicited output are dependent on PC processing. The motor effects of the BMRN, CBC, and SN units responsive to odor stimulation are unknown, so their activity cannot be used as yet to determine whether the odor stimulus was judged attractive or repellent by the preparation. Measurements of odor-elicited synaptic input to identified interneurons in the *Limax* feeding control circuit, such as the metacerebral giant cell (Chase and Tolloczko 1992; Egan and Gelperin 1981) or the feeding command cells (Delaney and Gelperin 1990c), may show differential activation by behaviorally attractive or repellent odors.

The ablation procedure used to test for PC processing during odor-elicited motor outputs used the contralateral nose after ablation to test that the response decrement after ipsilateral PC ablation was not due to nonspecific degradation in odor responsiveness of the preparation. The use of the contralateral nose is justified because although odor inputs are processed mainly unilaterally, the premotor and motor circuitry for feeding is strongly coupled bilaterally (Delaney and Gelperin 1990b) so that unilateral sensory inputs produce bilateral feeding motor activity (Culligan and Gelperin 1983). Reversible inactivation of PC processing can be accomplished with focal glutamate applications because glutamate inhibits the nonbursting PC cells (Gelperin et al. 1993), which constitute the largest fraction of cells in the PC lobe.

Relation to excitable systems

The issue of spatially coherent activity in nervous systems has considerable history, at least at the level of correlations between field potential measurements at two or more locations (Basar and Bullock 1989). However, the organization of neural activity as a slowly propagating front, pulse, or wave has been observed only in few systems, for example, the developing mammalian retina (Meister et al. 1991), the mammalian olfactory cortex (Ketchum and Haberly 1993), the central olfactory system of *Limax* (Delaney et al. 1994; Kleinfeld et al. 1994), in vitro preparations of mammalian thalamus and nucleus reticularis (Kim et al. 1995), and, in preliminary accounts, the olfactory bulb of frog (Delaney and Kleinfeld 1995) and the visual cortex of turtle (Precht et al. 1996). At present, the dynamics in *Limax* are unique in that the wavelength of the propagating pulse is clearly increased by external input (Delaney et al. 1994; Fig. 7), which can be thought of as the wavelength becoming much longer than the long axis of the PC. This is distinctly different from a simple increase in frequency of the PC oscillation, correlated with a decrease in period and wavelength. Thus the spatial pattern of the temporal dynamics is a signal that correlates with the presence of odor. It is an open question as to whether or not the animal makes use of this signal, as well as the odor dependence of the relative frequency of the underlying oscillation (Fig. 6), to formulate its behavior.

The electrical activity of the olfactory network in *Limax* appears to switch between the state with a propagating pulse to one with a stationary pulse (Delaney et al. 1994; Figs. 7 and 8). Such behavior may be generic to networks in which the length scale of inhibitory interactions is longer than that of the excitatory interactions (Krisher and Mikhailov 1994). The transition from the propagating to the stationary state

can be induced by a decrease in the time constant of the cells that make excitatory connections, presumably the non-bursting neurons in *Limax*, compared with that of the neurons that make inhibitory connections, presumably the bursting neurons. Such a change in time constant would result from olfactory input that depolarizes only nonbursting neurons, a possibility not inconsistent with the data.

We thank H. Sompolinsky and D. W. Tank for valuable discussions and J. A. Flores for assistance with data collection.

R. Gervais acknowledges support from the Centre National de la Recherche Scientifique and National Science Foundation Bursary. K. R. Delaney acknowledges support from National Sciences and Engineering Research Council Grant OGP0121698.

Present addresses: R. Gervais, Lab. Physiologie Neurosensorielle, Université Claude-Bernard Lyon-I, 69622 Villeurbanne, France; D. Kleinfeld, Dept. of Physics, University of California, La Jolla, CA 92093-0354; K. R. Delaney, Dept. of Biosciences, Simon Fraser University, Burnaby, BC V5A 1S6, Canada.

Address for reprint request: A. Gelperin, Rm. 1C464, Bell Laboratories, 600 Mountain Ave., Murray Hill, NJ 07974.

Received 29 June 1995; accepted in final form 7 February 1996.

REFERENCES

- ADRIAN, E. D. Olfactory reactions in the brain of the hedgehog. *J. Physiol. Lond.* 100: 459–473, 1942.
- BASAR, E. AND BULLOCK, T. H. *Brain Dynamics: Progress and Perspectives*. New York: Springer-Verlag, 1989.
- BERKOWICZ, D. A., TROMBLEY, P. Q., AND SHEPHERD, G. M. Evidence for glutamate as the olfactory receptor cell neurotransmitter. *J. Neurophysiol.* 71: 2557–2561, 1994.
- BEUERMANN, R. W. Slow potentials of the turtle olfactory bulb in response to odor stimulation of the nose. *Brain Res.* 97: 61–78, 1975.
- BREER, H. AND SHEPHERD, G. M. Implications of the NO/cGMP system for olfaction. *Trends Neurosci.* 16: 5–9, 1993.
- CHASE, R. AND HALL, B. Nociceptive inputs to C3, a motoneuron of the tentacle withdrawal reflex in *Helix aspersa*. *J. Comp. Physiol. A Sens. Neural Behav. Physiol.* In press.
- CHASE, R. AND TOLLOCZKO, B. Interganglionic dendrites constitute an output pathway from the procerobrum of the snail *Achatina fulica*. *J. Comp. Neurol.* 283: 143–152, 1989.
- CHASE, R. AND TOLLOCZKO, B. Synaptic innervation of the giant cerebral neuron in sated and hungry snails. *J. Comp. Neurol.* 318: 93–102, 1992.
- COPELAND, J. AND GELPERIN, A. Feeding and a serotonergic interneuron activate an identified autoactive salivary neuron in *Limax maximus*. *Comp. Biochem. Physiol. A Comp. Physiol.* 76: 21–30, 1983.
- CULLIGAN, N. AND GELPERIN, A. One-trial associative learning by an isolated molluscan CNS: use of different chemoreceptors for training and testing. *Brain Res.* 266: 319–327, 1983.
- DELANEY, K. AND GELPERIN, A. Cerebral interneurons controlling fictive feeding in *Limax maximus*. I. Anatomy and criteria for re-identification. *J. Comp. Physiol. A Sens. Neural Behav. Physiol.* 166: 297–310, 1990a.
- DELANEY, K. AND GELPERIN, A. Cerebral interneurons controlling fictive feeding in *Limax maximus*. II. Initiation and modulation of fictive feeding. *J. Comp. Physiol. A Sens. Neural Behav. Physiol.* 166: 311–326, 1990b.
- DELANEY, K. AND GELPERIN, A. Cerebral interneurons controlling fictive feeding in *Limax maximus*. III. Integration of sensory inputs. *J. Comp. Physiol. A Sens. Neural Behav. Physiol.* 166: 327–343, 1990c.
- DELANEY, K. R., GELPERIN, A., FEE, M. S., FLORES, J. A., GERVAIS, R., TANK, D. W., AND KLEINFELD, D. Waves and stimulus-modulated dynamics in an oscillating olfactory network. *Proc. Natl. Acad. Sci. USA* 91: 669–673, 1994.
- DELANEY, K. R. AND HALL, B. J. An in vitro nose-brain preparation of frog for the study of odor-induced oscillations in olfactory bulb and cortex. *J. Neurosci. Methods*. In press.
- DELANEY, K. R. AND KLEINFELD, D. Spatio-temporal dynamics of oscillatory activity in frog olfactory bulb. *Soc. Neurosci. Abstr.* 21: 1182, 1995.
- DIDIER, A., OTTERSEN, O. P., AND STORM-MATHISEN, J. Localization of taurine and glutamate in primary olfactory neurons in the rat. *Soc. Neurosci. Abstr.* 20: 1166, 1994.
- DORRIES, K. M., WHITE, J., AND KAUFER, J. S. A behavioral method for measuring olfactory discrimination in the tiger salamander. *Soc. Neurosci. Abstr.* 20: 331, 1994.
- EGAN, M. E. AND GELPERIN, A. Olfactory inputs to a bursting serotonergic interneuron in a terrestrial mollusc. *J. Molluscan Stud.* 47: 80–88, 1981.
- FREEMAN, W. J. *Mass Action in the Nervous System*. New York: Academic, 1975.
- FREEMAN, W. J. Nonlinear dynamics in olfactory information processing. In: *Olfaction: A Model System for Computational Neuroscience*, edited by J. L. Davis and H. Eichenbaum. Cambridge, MA: MIT Press, 1991, p. 225–249.
- FREEMAN, W. J. AND SCHNEIDER, W. S. Changes in spatial patterns of rabbit olfactory EEG with conditioning to odors. *Psychophysiology* 19: 44–56, 1982.
- FREEMAN, W. J. AND SKARDA, C. A. Spatial EEG patterns, nonlinear dynamics and perception: the neo-Sherringtonian view. *Brain Res. Rev.* 10: 147–175, 1985.
- FREEMAN, W. J. AND VIANA DI PRISCO, G. Relation of olfactory EEG to behavior: time series analysis. *Behav. Neurosci.* 100: 753–763, 1986.
- GELPERIN, A. Rapid food-aversion learning by a terrestrial mollusk. *Science Wash. DC* 189: 567–570, 1975.
- GELPERIN, A. Nitric oxide mediates network oscillations of olfactory interneurons in a terrestrial mollusc. *Nature Lond.* 369: 61–63, 1994.
- GELPERIN, A., GERVAIS, R., DELANEY, K., FEE, M. S., FLORES, J., TANK, D. W., AND KLEINFELD, D. Olfactory interneuron oscillations: optical and electrical measurements of intrinsic and odor-modulated activity. *Soc. Neurosci. Abstr.* 18: 303, 1992.
- GELPERIN, A., KLEINFELD, D., DENK, W., AND COOKE, I. R. C. Oscillations and gaseous oxides in invertebrate olfaction. *J. Neurobiol.* 30: 110–122, 1996.
- GELPERIN, A., RHINES, L., FLORES, J., AND TANK, D. W. Coherent network oscillations by olfactory interneurons: modulation by endogenous amines. *J. Neurophysiol.* 69: 1930–1939, 1993.
- GELPERIN, A. AND TANK, D. W. Odor-modulated collective network oscillations of olfactory interneurons in a terrestrial mollusc. *Nature Lond.* 345: 437–440, 1990.
- GRAY, C. M. AND SKINNER, J. E. Field potential response changes in the rabbit olfactory bulb accompany behavioral habituation during the repeated presentation of unreinforced odors. *Exp. Brain Res.* 73: 189–197, 1988.
- HABERLY, L. B. Olfactory cortex. In: *The Synaptic Organization of the Brain*, edited by G. M. Shepherd. New York: Oxford Univ. Press, 1990, p. 317–345.
- HILDEBRAND, J. G. Analysis of chemical signals by nervous systems. *Proc. Natl. Acad. Sci. USA* 92: 67–74, 1994.
- HOPFIELD, J. F. AND GELPERIN, A. Differential conditioning to a compound stimulus and its components in the terrestrial mollusc *Limax maximus*. *Behav. Neurosci.* 103: 274–293, 1989.
- HOPFIELD, J. J. Olfactory computation and object perception. *Proc. Natl. Acad. Sci. USA* 88: 6462–6466, 1991.
- KAUFER, J. S. Contributions of topography and parallel processing to odor coding in the vertebrate olfactory pathway. *Trends Neurosci.* 14: 79–85, 1991.
- KAY, L. M. AND FREEMAN, W. J. Coherence of gamma oscillations throughout olfactory and limbic brain structures in rats. *Soc. Neurosci. Abstr.* 20: 330, 1994.
- KETCHUM, K. AND HABERLY, L. B. Synaptic events that generate fast oscillations in piriform cortex. *J. Neurosci.* 13: 3980–3985, 1993.
- KIM, V., BAL, T., AND MCCORMICK, D. A. Spindle waves are propagating synchronized oscillations in the ferret LGNd in vitro. *J. Neurophysiol.* 74: 1301–1323, 1995.
- KIMURA, T., SUZUKI, B., YAMADA, A., SEKIGUCHI, T., AND MIZUKAMI, A. Response of oscillatory field potential to some conditioned odors in slug's brain (Abstract). *Zool. Sci.* 9: 1241, 1993.
- KLEINFELD, D., DELANEY, K. R., FEE, M. S., FLORES, J. A., TANK, D. W., AND GELPERIN, A. Dynamics of propagating waves in the olfactory network of a terrestrial mollusc: an electrical and optical study. *J. Neurophysiol.* 72: 1402–1419, 1994.
- KRISHER, K. AND MIKHAILOV, A. Bifurcation to traveling spots in reaction-diffusion systems. *Phys. Rev. Lett.* 73: 3165–3168, 1994.
- LANCET, D. Exclusive receptors. *Nature Lond.* 372: 321–322, 1994.
- LASSER-ROSS, N., MIYAKAWA, H., LEV-RAM, V., YOUNG, S. R., AND ROSS, W. N. High time resolution fluorescence imaging with a CCD camera. *J. Neurosci. Methods* 26: 253–261, 1991.
- LAURENT, G. AND DAVIDOWITZ, H. Encoding of olfactory information with oscillating neural assemblies. *Science Wash. DC* 265: 1872–1875, 1994.

- LAURENT, G. AND NARAGHI, M. Odorant-induced oscillations in the mushroom bodies of the locust. *J. Neurosci.* 14: 2993–3004, 1994.
- LIBET, B. AND GERARD, R. W. Control of the potential rhythm of the isolated frog brain. *J. Neurophysiol.* 2: 153–169, 1939.
- LOEW, L. M., COHEN, L. B., DIX, J., FLUHLER, E. N., MONTANA, V., SALAMA, G., AND WU, J. Y. A naphthyl analog of the aminostyryl pyridinium class of potentiometric membrane dyes shows consistent sensitivity in a variety of tissue, cell and model membrane preparations. *J. Membr. Biol.* 130: 1–10, 1992.
- MEISTER, M., WONG, R. O., BAYLOR, D. A., AND SHATZ, C. J. Synchronous bursts of action potentials in ganglion cells of the developing mammalian retina. *Science Wash. DC* 252: 939–943, 1991.
- MELLON, D., SANDEMAN, D. C., AND SANDEMAN, R. E. Characterization of oscillatory olfactory interneurons in the protocerebrum of the crayfish. *J. Exp. Biol.* 167: 15–38, 1992.
- MORI, K. AND SHEPHERD, G. M. Emerging principles of molecular signal processing by mitral/tufted cells in the olfactory bulb. *Semin. Cell Biol.* 5: 65–74, 1994.
- PESCHEL, M., STRAUB, V., AND TEYKE, T. Consequences of food-attraction conditioning in *Helix*: a behavioral and electrophysiological study. *J. Comp. Physiol. A Sens. Neural Behav. Physiol.* 178: 317–327, 1996.
- PRECHTL, J. C., COHEN, L. B., MITRA, P. P., AND KLEINFELD, D. Spatio-temporal structure of stimulus induced electrical activity in turtle visual cortex. *Soc. Neurosci. Abstr.* In press.
- PRIOR, D. AND GELPERIN, A. Autoactive molluscan neuron: reflex function and synaptic modulation during feeding in the terrestrial slug *Limax maximus*. *J. Comp. Physiol.* 114: 217–232, 1977.
- ROSKAMS, A. J., BREDET, D. S., DAWSON, T. M., AND RONNETT, G. V. Nitric oxide mediates the formation of synaptic connections in developing and regenerating olfactory receptor neurons. *Neuron* 13: 289–299, 1994.
- SAHLEY, C. L. The behavioral analysis of associative learning in the terrestrial mollusc *Limax maximus*: the importance of interevent relationships. In: *Connectionist Modeling and Brain Function: The Developing Interface*, edited by S. Hanson and C. Olson. Cambridge, MA: MIT Press, 1990, p. 36–73.
- SAHLEY, C. L., MARTIN, K. A., AND GELPERIN, A. Analysis of associative learning in the terrestrial mollusc *Limax maximus*. II. Appetitive learning. *J. Comp. Physiol. A Sens. Neural Behav. Physiol.* 167: 339–345, 1990.
- SAHLEY, C. L., MARTIN, K. A., AND GELPERIN, A. Odors can induce feeding motor responses in the terrestrial mollusc *Limax maximus*. *Behav. Neurosci.* 106: 563–568, 1992.
- SALZBERG, B. M., OBAID, A. L., SENSEMAN, D. M., AND GAINER, H. Optical recording of action potentials from vertebrate nerve terminals using potentiometric probes provides evidence for sodium and calcium compartments. *Nature Lond.* 306: 36–40, 1983.
- SASSOE-POGNETTO, M., CANTINO, D., PANZANELLI, P., VERDUN DI CANTOGNO, L., GIUSTETTO, M., MARGOLIS, F. L., DE BIASI, S., AND FASOLO, A. Presynaptic colocalization of carnosine and glutamate in olfactory neurons. *Neuroreport* 5: 7–10, 1993.
- SATOU, M. Synaptic organization, local neuronal circuitry, and functional segregation of the teleost olfactory bulb. *Prog. Neurobiol.* 34: 115–142, 1990.
- SCHÜTT, A. AND BASAR, E. Olfactory field potential oscillations in the isolated *Helix* brain: different odors induce different rhythmicities. *Abstr. 39th Mtg. German EEG Soc.* p. 184, 1994.
- SKINNER, J. E., MARTIN, J. L., LANDISMAN, C. E., MOMMER, M. M., FULTON, K., MITRA, M., BURTON, W. D., AND SALTZBERG, B. Chaotic attractors in a model of neocortex: dimensionalities of olfactory bulb surface potentials are spatially uniform and event related. In: *Chaos in Brain Function*, edited by E. Basar. Berlin: Springer-Verlag, 1990, p. 119–134.
- TANK, D. W., GELPERIN, A., AND KLEINFELD, D. Odors, oscillations, and waves: does it all compute? *Science Wash. DC* 265: 1819–1820, 1994.
- THOMMESSEN, G. The spatial distribution of odor-induced potentials in the olfactory bulb of char and trout (*Salmonidae*). *Acta Physiol. Scand.* 102: 205–217, 1978.
- VIANA DI PRISCO, G. AND FREEMAN, W. J. Odor-related bulbar EEG spatial pattern analysis during appetitive conditioning in rabbits. *Behav. Neurosci.* 99: 964–978, 1985.
- YAMADA, A., KIMURA, T., IWAMA, A., SUZUKI, Y., KAWAHARA, S., KIRINO, Y., AND SEKIGUCHI, T. A study of interactions between olfaction and taste in the central nervous system of a slug. *Soc. Neurosci. Abstr.* In press.